# Automated and High-Speed Packaging System

# 9

## 9.1 Design of Automated and High-Speed Packaging Machinery System

The automated packing machinery becomes more popular in many different industries to reduce labor cost. This new packaging machinery system can automatically load carton papers, open carton paper to the square box, seal the bottom flap, seal top flap after putting the products into box, label print, and offload the packing box to the loading area in the production line. Figure 9.1 shows the layout of this new automated packaging assembly system. The details of full packaging production sequence of this new packaging system are described as follows:

The carton papers are loaded into the loading channel and each carton paper is sucked into the production inline from loading channel by vacuum cup. There is a support plate at the front of vacuum cup and support plate is aligned with carton paper. The carton paper falls down before vacuum cup picks it up. The soft spring leaf in support plate can keep carton paper fixed while opening square box. At each side of box bottom, there are two movable pushing plates that first move up to flatten two box short flaps and flatten two long flaps thereafter. Two pushing plates move to the left or the right separately and the box bottom is finally sealed by bottom sealing mechanism. After sealing the box bottom, a pushing plate at the left side will drive box to the next station to print label at two sides of box. A support plate at the top of packing box is to make sure that the labels printed at two sides are horizontal with no titled angle. To close and seal the top flaps of packing box after loading the products, three mechanisms can be introduced including divider, pusher, and final curvature. Before packing box moving to contact final curvature, the divider separates long flaps of box top into two sides to keep them staying with the wall with no contact with short flaps. The box continues to move from the left to the right until it contacts the final curvature. The final curvatures are used for final closing of packing box at the top and the curvature will close the flaps at the box top gradually. There are two curvatures in final curvature mechanism: front curvature and rear curvature. The front curvature is applied to push down the short flaps and simultaneously separate



J. Zheng Li, *CAD, 3D Modeling, Engineering Analysis, and Prototype Experimentation*, DOI 10.1007/978-3-319-05921-1_9

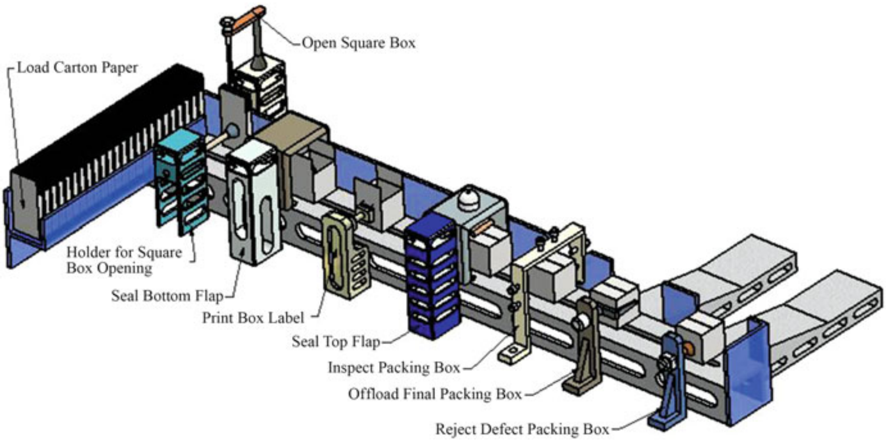


**Fig. 9.1** Fully automated packaging assembly system

long flaps. This curvature is combined with two vertically and one horizontally changed curvatures to keep gradual closing of short flaps. The rear curvature is applied to gradually close two long flaps. The offloading mechanism is to load finished packing box to the product loading area and rejecting mechanism is to reject the packing box if some defects occurred during packing process.

## 9.2 Computer-Aided Simulation on Automated and High-Speed Packaging Machinery System

There are various loading forces generated during automated packaging processes including vibration, insertion, and packing. The computer-aided modeling and simulation are applied to diagnose the mechanism function and verify the component strength for solid performance. The vibration is caused by different forces including mass inertia and internal shocking forces during kinematic movement. The mathematical modeling shows the following equation (Isaev et al. 2005; Kundu and Cohen 2008):

$$M(F) = \frac{B_{\mathrm{BF}}(F)}{B_{\mathrm{OD}}(F)} = \frac{M''(F)}{M'(F)} \tag{9.1}$$

Here, $M'(F) = \frac{B_{\mathrm{OD}}(F)}{D_{\mathrm{P}}(F)}$ and $M''(F) = \frac{B_{\mathrm{BF}}(F)}{D_{\mathrm{P}}(F)}$.

$D_{\mathrm{P}}(F)$—Fourier transform of pushing device.

$B_{\mathrm{OD}}(F)$—Fourier transform of output delivery moving acceleration.

$B_{\mathrm{BF}}(F)$—Fourier transform of base frame acceleration.

Figures 9.2, 9.3, 9.4, 9.5, 9.6, 9.7, 9.8, 9.9, 9.10, 9.11, 9.12, 9.13, 9.14, 9.15, 9.16, 9.17, 9.18, 9.19, 9.20, 9.21, 9.22, 9.23, 9.24, 9.25, and 9.26 display the computational simulation results in this new automated and high-speed packaging system.

**Fig. 9.2** Carton loading unit

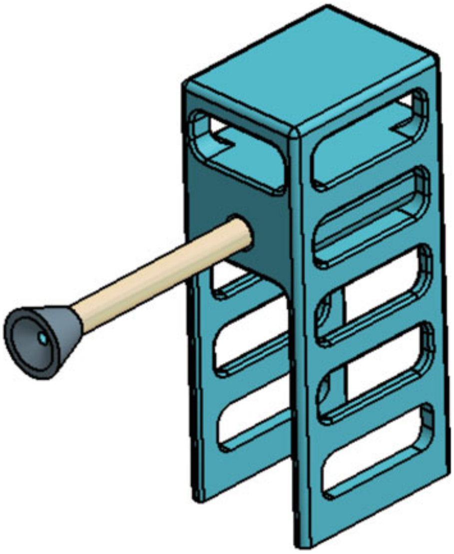

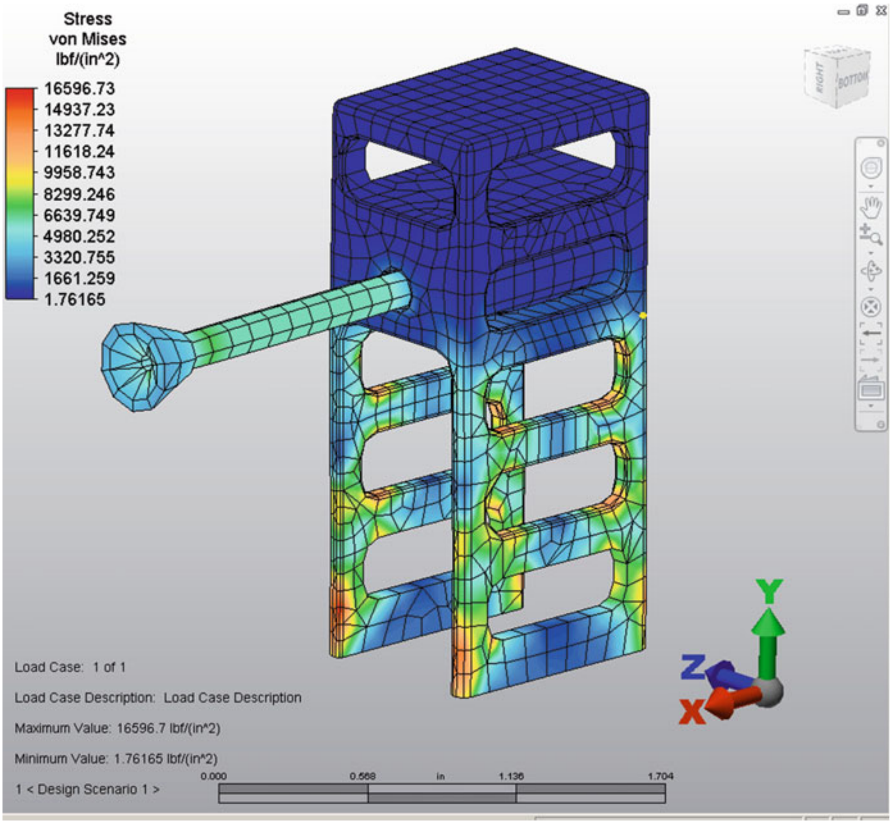


**Fig. 9.3** Stress profile in carton loading unit

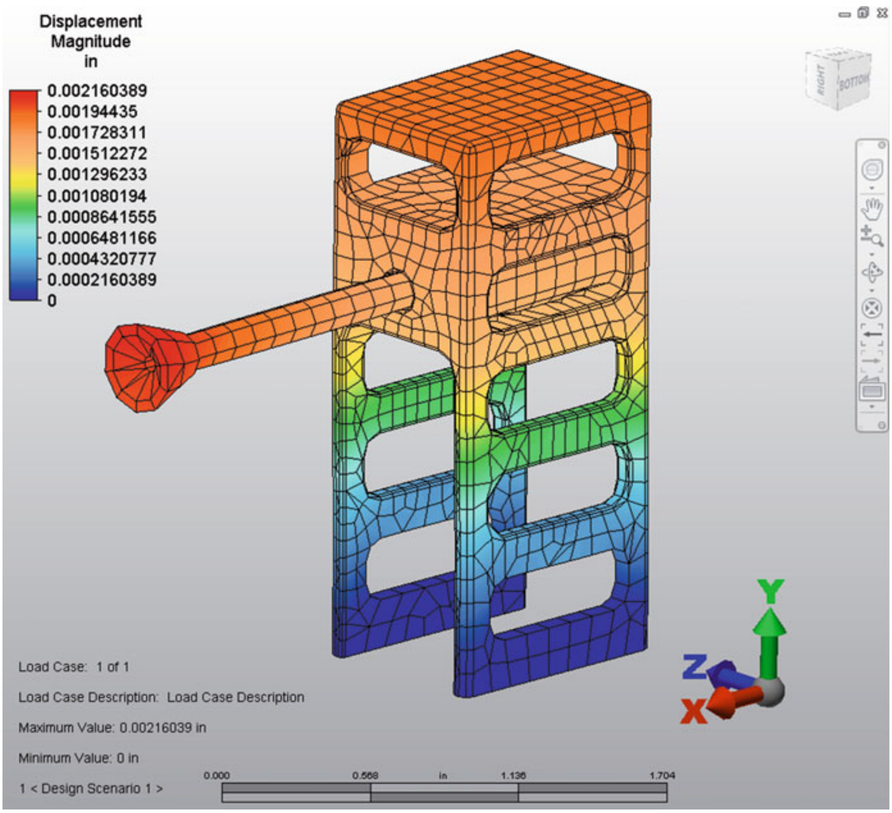


**Fig. 9.4** Deflection profile in carton loading unit

**Fig. 9.5** Carton separating unit

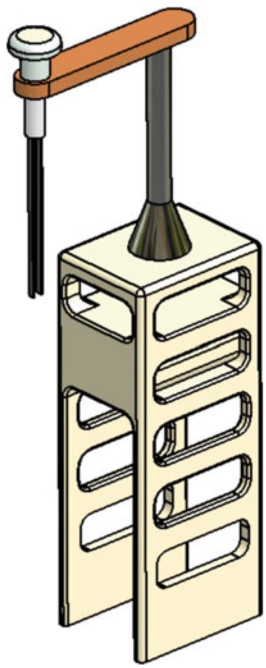

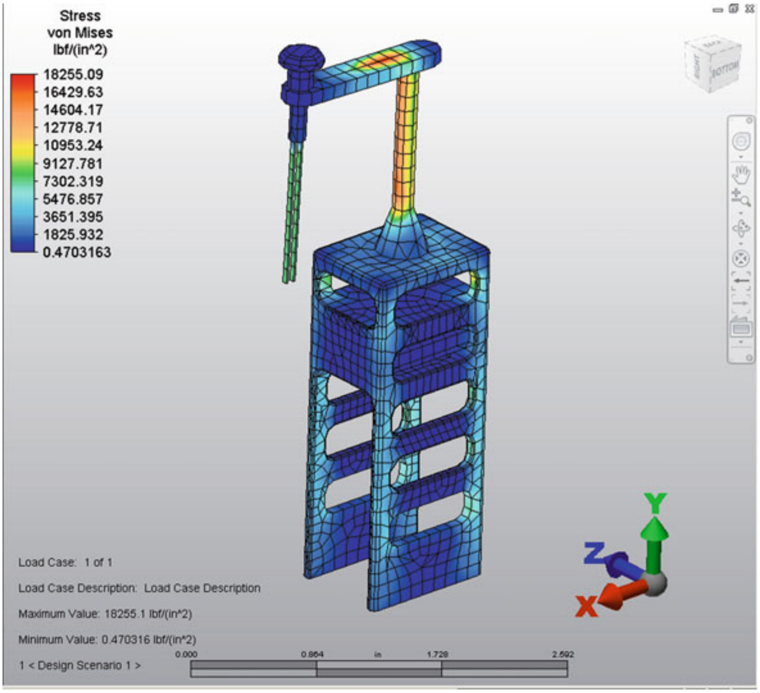


**Fig. 9.6** Stress profile in carton separating unit

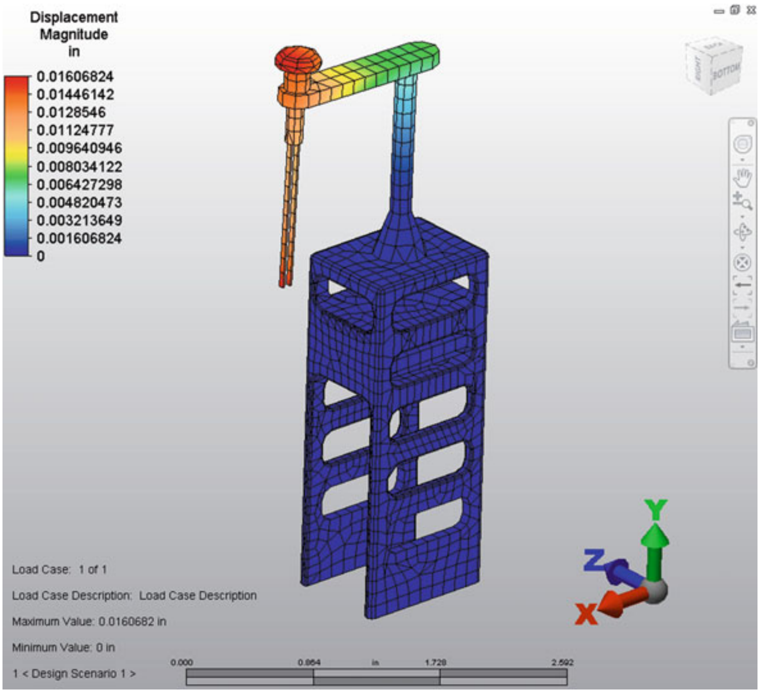


**Fig. 9.7** Deflection profile in carton separating unit

**Fig. 9.8** Carton bottom closer

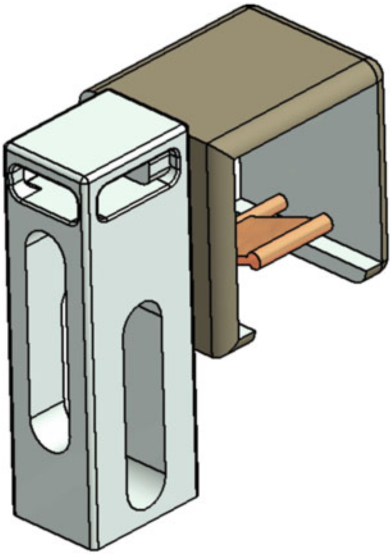

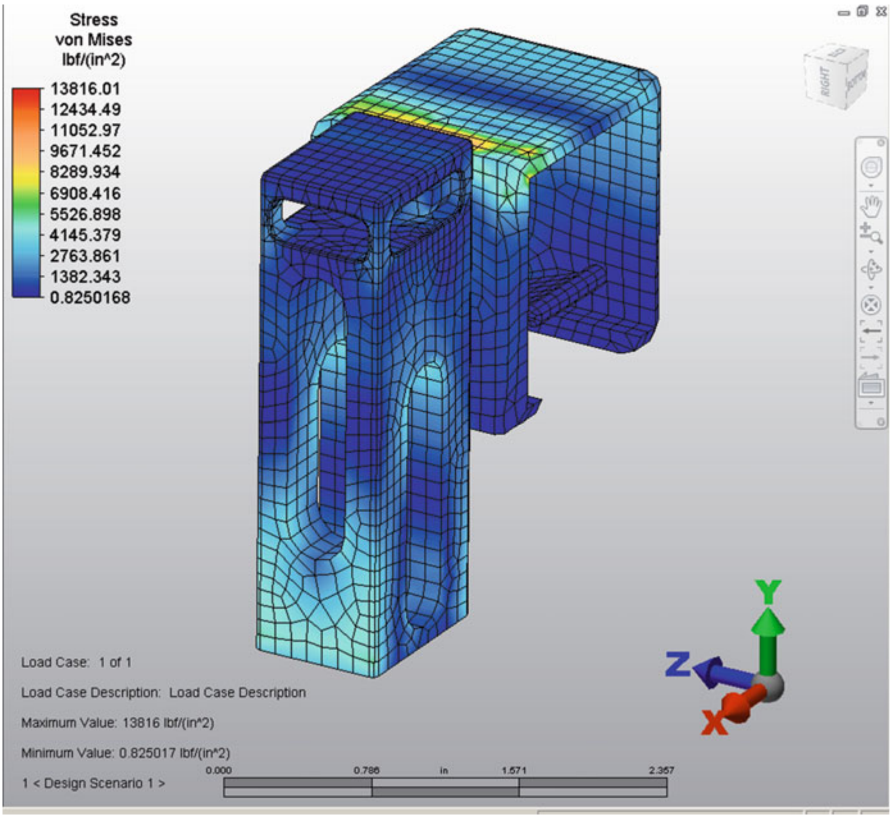


**Fig. 9.9** Stress profile at base support in carton bottom closer

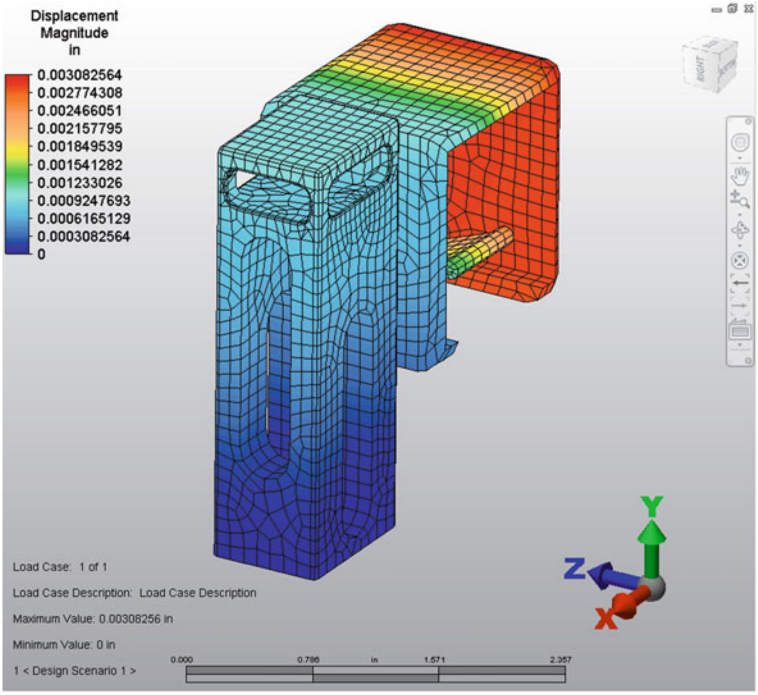


**Fig. 9.10** Deflection profile at base support in carton bottom closer

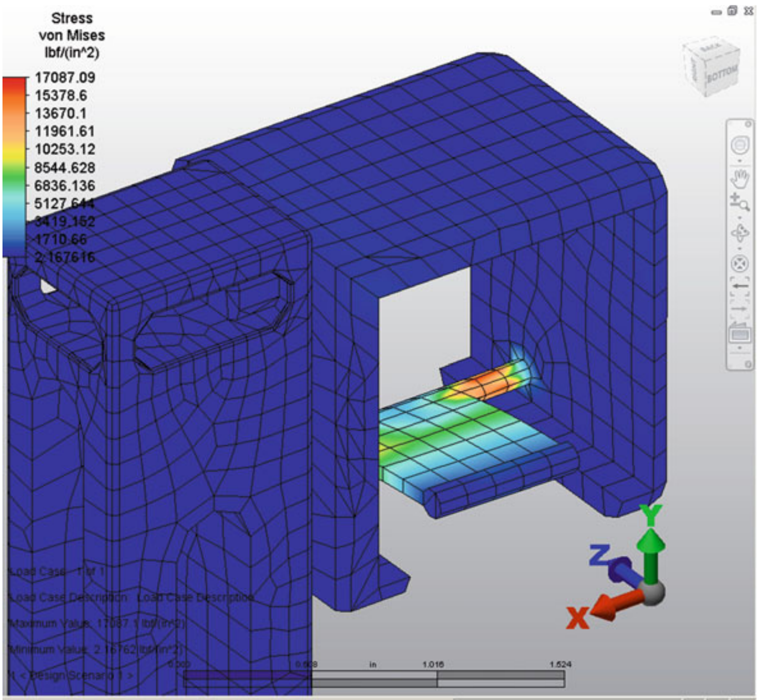


**Fig. 9.11** Stress profile at tension mechanism in carton bottom closer

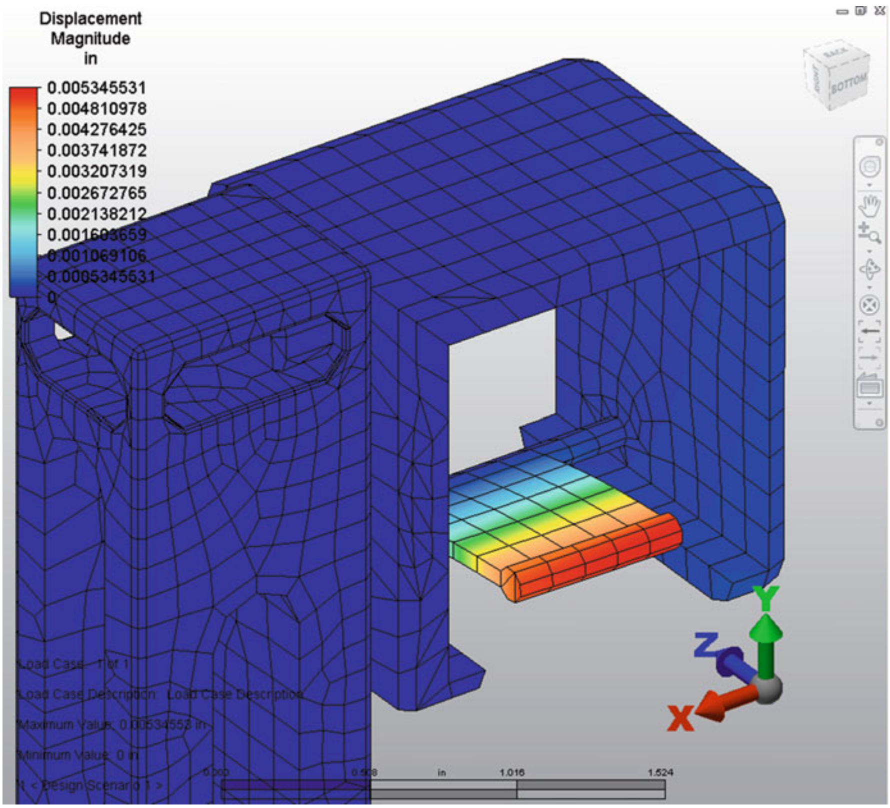


**Fig. 9.12** Deflection profile at tension mechanism in carton bottom closer

**Fig. 9.13** Labeling unit

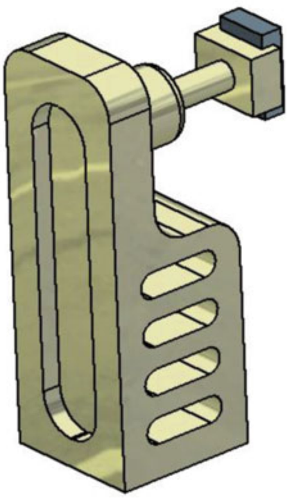

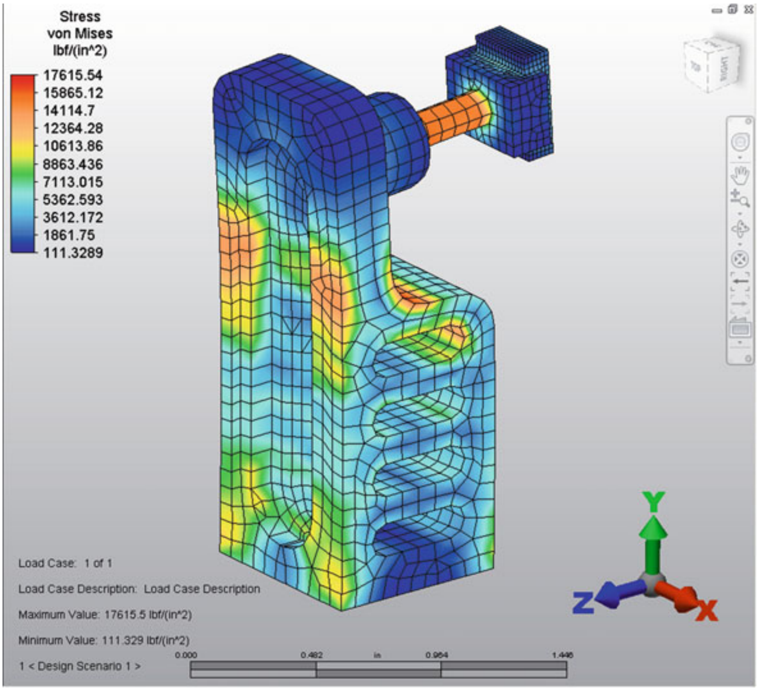


**Fig. 9.14** Stress profile in labeling unit

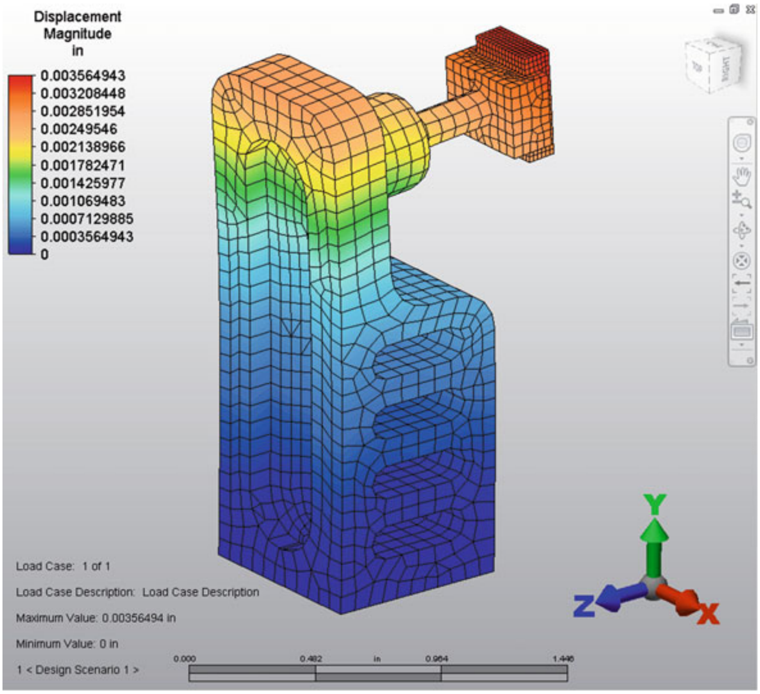


**Fig. 9.15** Deflection profile in labeling unit

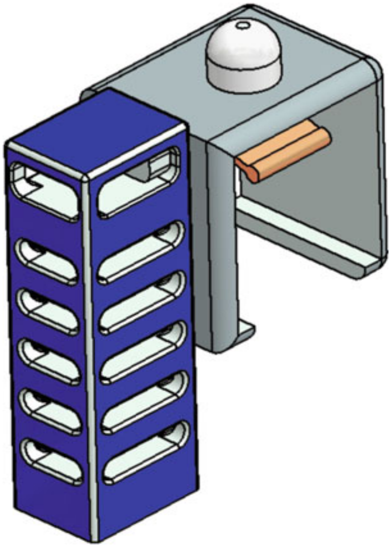

**Fig. 9.16** Carton top closer

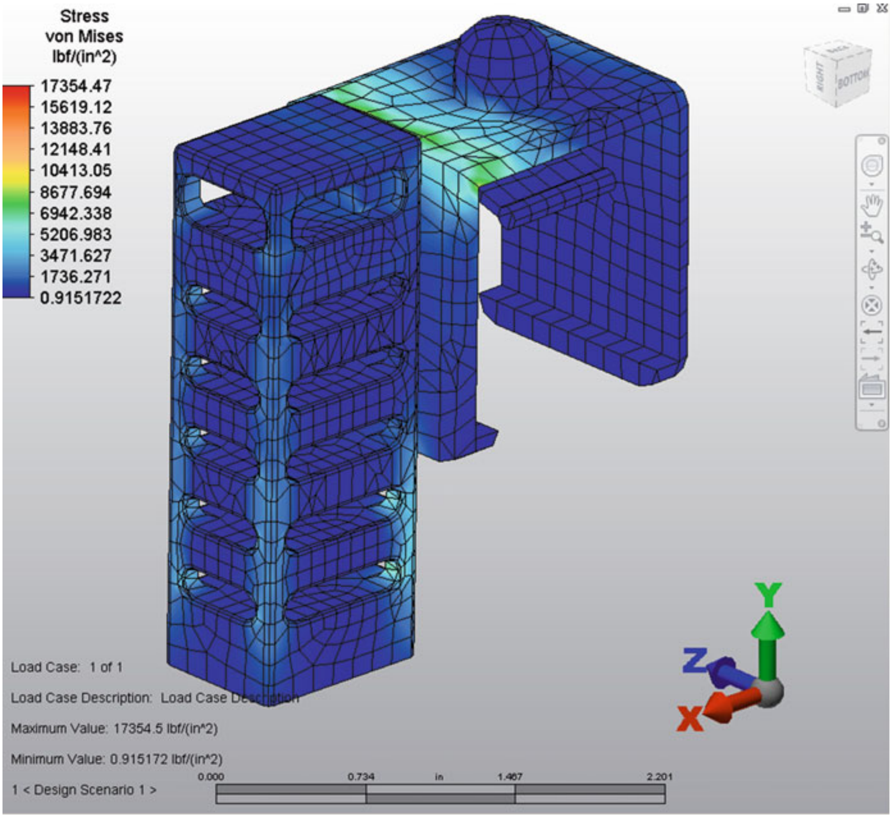


**Fig. 9.17** Stress profile at base support in carton top closer

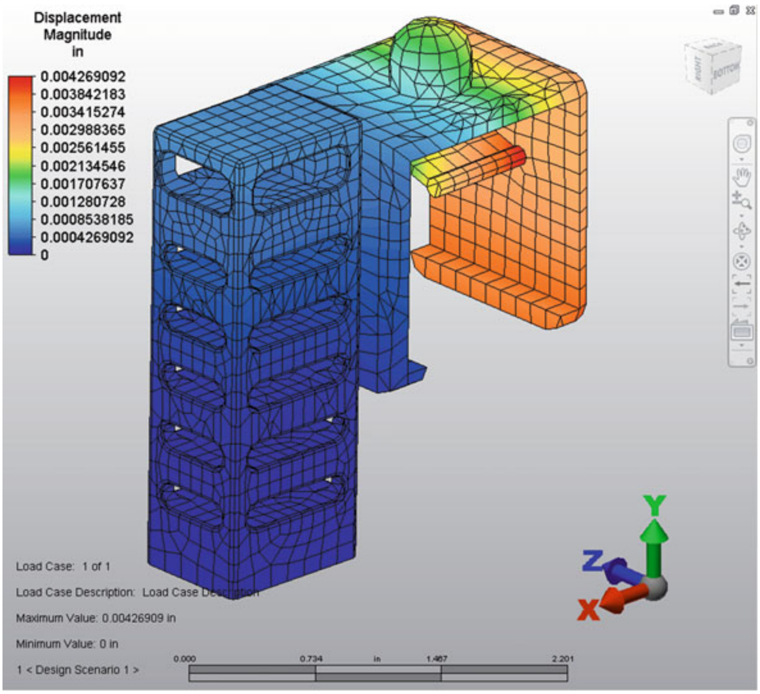


**Fig. 9.18** Deflection profile at base support in carton top closer

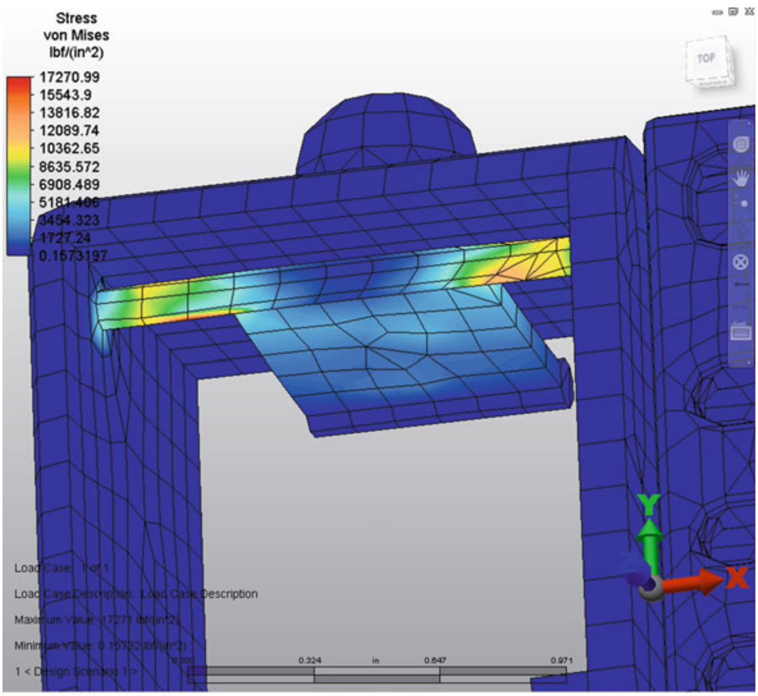


**Fig. 9.19** Stress profile at tension mechanism in carton top closer

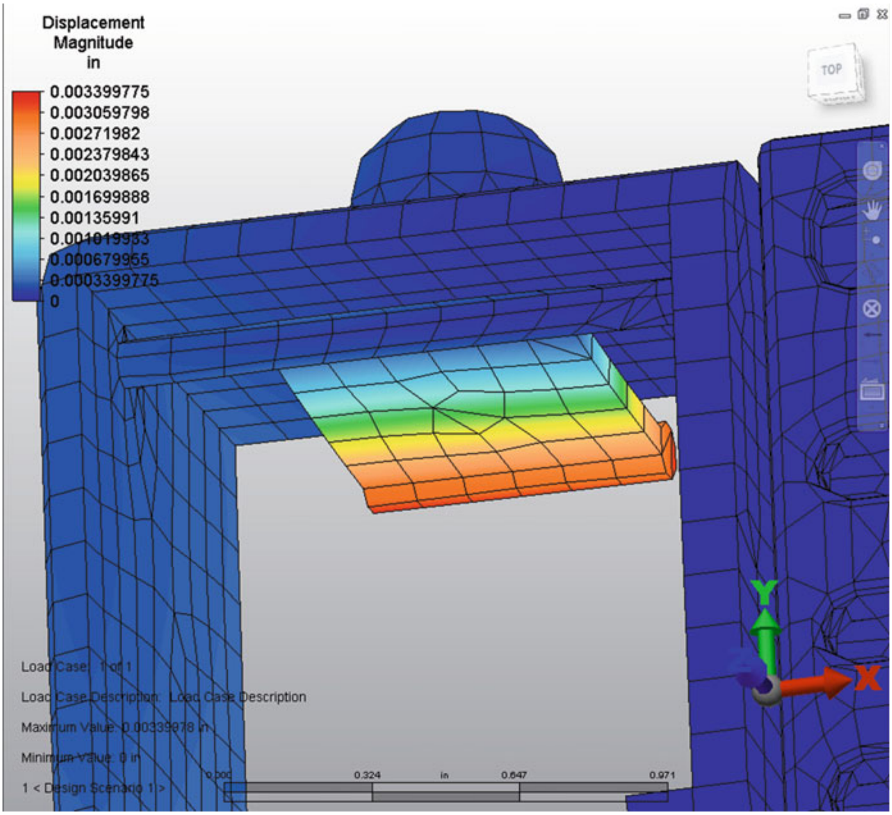


**Fig. 9.20** Deflection profile at tension mechanism in carton top closer

**Fig. 9.21** Offloading unit

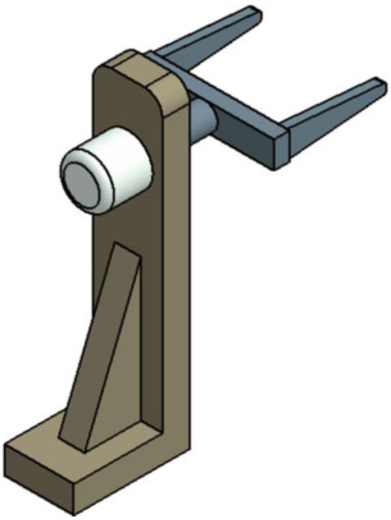

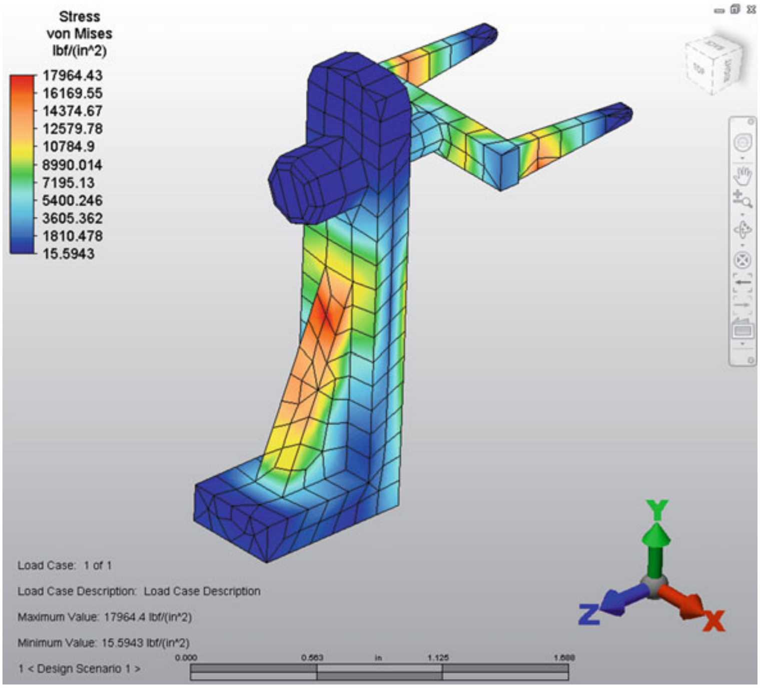


**Fig. 9.22** Stress profile in offloading unit

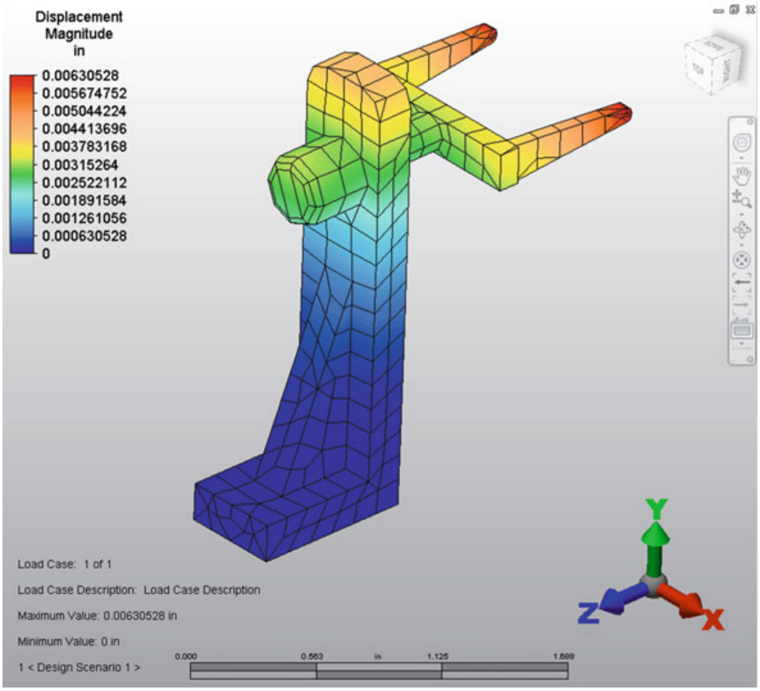


**Fig. 9.23** Deflection profile in offloading unit

**Fig. 9.24** Rejecting unit

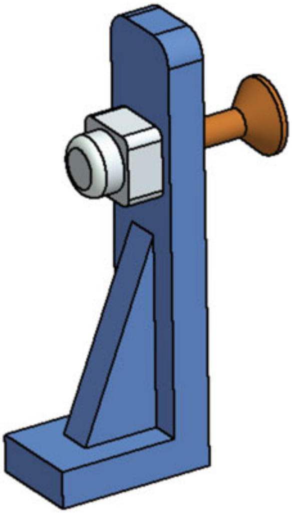

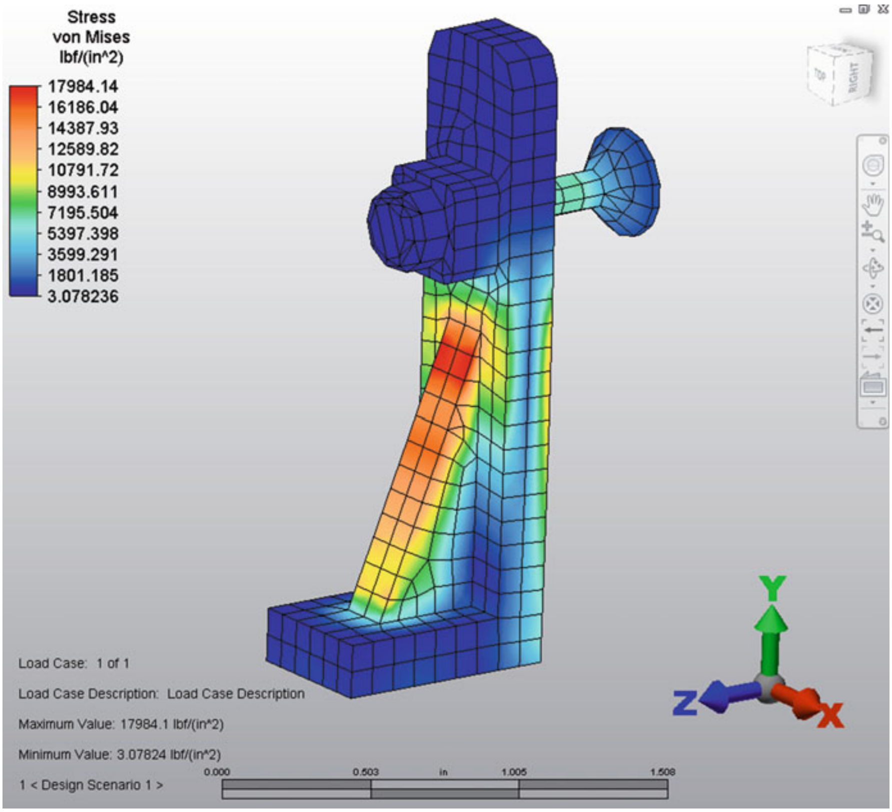


**Fig. 9.25** Stress profile in rejecting unit

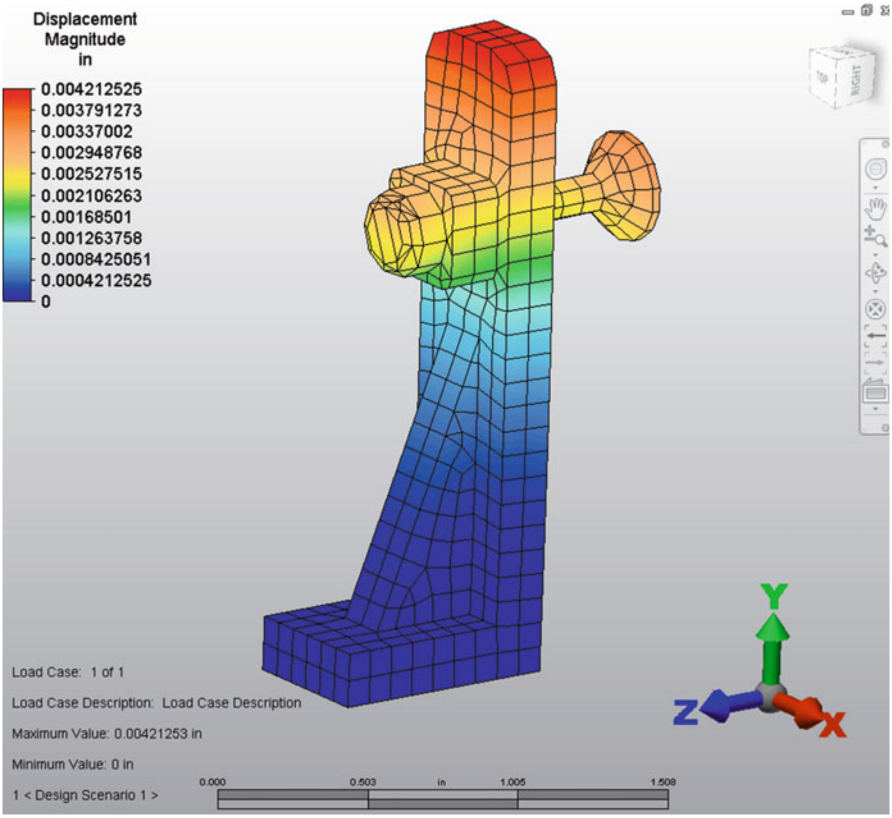


**Fig. 9.26** Deflection profile in rejecting unit

The computer-aided simulation and analysis in Figs. 9.3 and 9.4 present the stress and deflection of carton loading unit in this new automated and high-speed packaging system. The analytic results demonstrate that the maximum stress of 16,596.73 psi in this carton loading unit is less than the material yield strength of 36,000 psi and maximum deflection of 0.00216 in. is within material allowable deflection limit.

The computer-aided simulation and analysis in Figs. 9.6 and 9.7 indicate the stress and deflection of carton separating unit in this new automated and high-speed packaging system. The analytic results state that the maximum stress of 18,255.09 psi in this carton separating unit is less than the material yield strength of 36,000 psi and maximum deflection of 0.01607 in. is within material allowable deflection limit.

The computer-aided simulation and analysis in Figs. 9.9 and 9.10 indicate the stress and deflection of carton bottom closer in this new automated and high-speed packaging system. The analytic results state that the maximum stress of 13,816.01 psi in this carton bottom closer is less than the material yield strength of 36,000 psi and maximum deflection of 0.00308 in. is within material allowable deflection limit.

The computer-aided simulation and analysis in Figs. 9.11 and 9.12 indicate the stress and deflection of tension mechanism in carton bottom closer. The analytic results state that the maximum stress of 17,087.09 psi in this tension mechanism is less than the material yield strength of 36,000 psi and maximum deflection of 0.00535 in. is within material allowable deflection limit.

The computer-aided simulation and analysis in Figs. 9.14 and 9.15 indicate the stress and deflection of labeling unit in this new automated and high-speed packaging system. The analytic results state that the maximum stress of 17,615.54 psi in this labeling unit is less than the material yield strength of 36,000 psi and maximum deflection of 0.00356 in. is within material allowable deflection limit.

The computer-aided simulation and analysis in Figs. 9.17 and 9.18 indicate the stress and deflection of base support of carton top closer in this new automated and high-speed packaging system. The analytic results state that the maximum stress of 17,354.47 psi in this base support is less than the material yield strength of 36,000 psi and maximum deflection of 0.00427 in. is within material allowable deflection limit.

The computer-aided simulation and analysis in Figs. 9.19 and 9.20 indicate the stress and deflection of tension mechanism of carton top closer in this new automated and high-speed packaging system. The analytic results state that the maximum stress of 17,270.99 psi in this tension mechanism of carton top closer is less than the material yield strength of 36,000 psi and maximum deflection of 0.00339 in. is within material allowable deflection limit.

The computer-aided simulation and analysis in Figs. 9.22 and 9.23 indicate the stress and deflection of offloading unit in this new automated and high-speed packaging system. The analytic results state that the maximum stress of 17,964.43 psi in this offloading unit is less than the material yield strength of 36,000 psi and maximum deflection of 0.00631 in. is within material allowable deflection limit.

The computer-aided simulation and analysis in Figs. 9.25 and 9.26 indicate the stress and deflection of rejecting unit in this new automated and high-speed packaging system. The analytic results state that the maximum stress of 17,984.14 psi in this rejecting unit is less than the material yield strength of 36,000 psi and maximum deflection of 0.00421 in. is within material allowable deflection limit.

The above computational simulation results displayed in these figures show that the maximum stresses on these important components are all less than the material yield stress and maximum material deflections are all within material allowable deformation limits. The computational solutions confirm that this newly developed automated and high-speed packaging system works well in packaging applications.

## 9.3 Experiment on Automated and High-Speed Packaging Machinery System

The newly designed automated and high-speed packaging machinery system has been prototyped and tested to compare and verify the results from computer-aided simulation. Table 9.1 demonstrates the prototype testing results of carton loading unit in this new automated and high-speed packaging machinery system.

The prototype experimental results of carton loading unit in Table 9.1 verify the proper function because the average maximum stress 16,595.84 psi and average maximum deflection 0.00242 in. are close to the results of maximum stress 16,596.73 psi and maximum deflection 0.00216 in. that are represented, respectively, in Figs. 9.3 and 9.4 by computer-aided modeling and numerical simulation.

Table 9.2 expresses the prototype testing results of carton separating unit in this new automated and high-speed packaging machinery system.

The prototype experimental results of carton separating unit in Table 9.2 confirm the appropriate function since the average maximum stress 18,255.72 psi and average maximum deflection 0.01656 in. are similar to the results of maximum stress 18,255.09 psi and maximum deflection 0.01607 in. that are indicated, respectively, in Figs. 9.6 and 9.7 by computer-aided modeling and numerical simulation.

Table 9.3 records the prototype testing results of base support of carton bottom closer unit in this new automated and high-speed packaging machinery system.

**Table 9.1** Prototype testing of carton loading unit in this new automated and high-speed packaging machinery system

| Number of experiment | Maximum stress (psi) | Maximum deflection (in.) |
|---|---|---|
| 1 | 16,595.78 | 0.00238 |
| 2 | 16,596.65 | 0.00256 |
| 3 | 16,594.38 | 0.00208 |
| 4 | 16,595.88 | 0.00255 |
| 5 | 16,596.98 | 0.00268 |
| 6 | 16,596.48 | 0.00212 |
| 7 | 16,596.55 | 0.00205 |
| 8 | 16,596.24 | 0.00286 |
| 9 | 16,594.95 | 0.00211 |
| 10 | 16,595.18 | 0.00202 |
| 11 | 16,596.35 | 0.00278 |
| 12 | 16,594.88 | 0.00266 |
| 13 | 16,595.18 | 0.00298 |
| 14 | 16,596.48 | 0.00206 |
| 15 | 16,594.65 | 0.00201 |
| 16 | 16,596.26 | 0.00256 |
| 17 | 16,596.59 | 0.00299 |
| 18 | 16,594.68 | 0.00245 |
| 19 | 16,596.22 | 0.00206 |
| 20 | 16,596.45 | 0.00236 |
| Average | 16,595.84 | 0.00242 |

**Table 9.2** Prototype testing of carton separating unit in this new automated and high-speed packaging machinery system

| Number of experiment | Maximum stress (psi) | Maximum deflection (in.) |
|---|---|---|
| 1 | 18,256.38 | 0.01655 |
| 2 | 18,254.99 | 0.01588 |
| 3 | 18,255.59 | 0.01678 |
| 4 | 18,254.88 | 0.01599 |
| 5 | 18,255.18 | 0.01697 |
| 6 | 18,256.01 | 0.01678 |
| 7 | 18,255.09 | 0.01698 |
| 8 | 18,256.18 | 0.01638 |
| 9 | 18,255.48 | 0.01684 |
| 10 | 18,255.78 | 0.01678 |
| 11 | 18,256.35 | 0.01688 |
| 12 | 18,254.89 | 0.01598 |
| 13 | 18,255.85 | 0.01668 |
| 14 | 18,256.48 | 0.01695 |
| 15 | 18,255.88 | 0.01684 |
| 16 | 18,256.68 | 0.01597 |
| 17 | 18,254.99 | 0.01685 |
| 18 | 18,256.84 | 0.01678 |
| 19 | 18,254.98 | 0.01593 |
| 20 | 18,255.88 | 0.01648 |
| Average | 18,255.72 | 0.01656 |

**Table 9.3** Prototype testing of base support of carton bottom closer unit in this new automated and high-speed packaging machinery system

| Number of experiment | Maximum stress (psi) | Maximum deflection (in.) |
|---|---|---|
| 1 | 13,816.01 | 0.00338 |
| 2 | 13,816.01 | 0.00304 |
| 3 | 13,815.38 | 0.00298 |
| 4 | 13,816.08 | 0.00368 |
| 5 | 13,815.18 | 0.00355 |
| 6 | 13,815.25 | 0.00299 |
| 7 | 13,816.11 | 0.00388 |
| 8 | 13,815.08 | 0.00398 |
| 9 | 13,816.15 | 0.00297 |
| 10 | 13,815.02 | 0.00378 |
| 11 | 13,815.18 | 0.00389 |
| 12 | 13,815.04 | 0.00395 |
| 13 | 13,816.15 | 0.00378 |
| 14 | 13,815.18 | 0.00296 |
| 15 | 13,815.06 | 0.00388 |
| 16 | 13,816.08 | 0.00393 |
| 17 | 13,815.15 | 0.00397 |
| 18 | 13,815.08 | 0.00298 |
| 19 | 13,815.12 | 0.00396 |
| 20 | 13,816.18 | 0.00388 |
| Average | 13,815.52 | 0.00357 |

**Table 9.4** Prototype testing of tension mechanism of carton bottom closer unit in this new automated and high-speed packaging machinery system

| Number of experiment | Maximum stress (psi) | Maximum deflection (in.) |
|---|---|---|
| 1 | 17,087.02 | 0.00502 |
| 2 | 17,087.88 | 0.00555 |
| 3 | 17,088.89 | 0.00499 |
| 4 | 17,088.55 | 0.00508 |
| 5 | 17,086.88 | 0.00505 |
| 6 | 17,087.99 | 0.00575 |
| 7 | 17,086.98 | 0.00498 |
| 8 | 17,087.85 | 0.00438 |
| 9 | 17,087.98 | 0.00525 |
| 10 | 17,086.78 | 0.00478 |
| 11 | 17,087.68 | 0.00418 |
| 12 | 17,087.79 | 0.00556 |
| 13 | 17,086.78 | 0.00448 |
| 14 | 17,087.84 | 0.00418 |
| 15 | 17,086.97 | 0.00435 |
| 16 | 17,087.84 | 0.00448 |
| 17 | 17,087.98 | 0.00505 |
| 18 | 17,087.88 | 0.00435 |
| 19 | 17,086.78 | 0.00438 |
| 20 | 17,087.75 | 0.00538 |
| Average | 17,087.60 | 0.00486 |

The prototype experimental results for base support of carton bottom closer unit in Table 9.3 prove the normal function as the average maximum stress 13,815.52 psi and average maximum deflection 0.00357 in. are almost equal to the results of maximum stress 13,816.01 psi and maximum deflection 0.00308 in. that are laid out, respectively, in Figs. 9.9 and 9.10 by computer-aided modeling and numerical simulation.

Table 9.4 states the prototype testing results of tension mechanism of carton bottom closer unit in this new automated and high-speed packaging machinery system.

The prototype experimental results for tension mechanism of carton bottom closer unit in Table 9.4 verify the proper function because the average maximum stress 17,087.60 psi and average maximum deflection 0.00486 in. are very similar to the results of maximum stress 17,087.09 psi and maximum deflection 0.00535 in. that are shown, respectively, in Figs. 9.11 and 9.12 by computer-aided modeling and numerical simulation.

Table 9.5 demonstrates the prototype testing results of labeling unit in this new automated and high-speed packaging machinery system.

The prototype experimental results of labeling unit in Table 9.5 confirm the appropriate function since the average maximum stress 17,616.12 psi and average maximum deflection 0.00314 in. are closely equal to the results of maximum stress

**Table 9.5** Prototype testing of labeling unit in this new automated and high-speed packaging machinery system

| Number of experiment | Maximum stress (psi) | Maximum deflection (in.) |
|---|---|---|
| 1 | 17,616.48 | 0.00318 |
| 2 | 17,615.38 | 0.00377 |
| 3 | 17,616.84 | 0.00308 |
| 4 | 17,616.78 | 0.00305 |
| 5 | 17,615.29 | 0.00268 |
| 6 | 17,616.98 | 0.00368 |
| 7 | 17,615.44 | 0.00278 |
| 8 | 17,616.68 | 0.00301 |
| 9 | 17,616.68 | 0.00367 |
| 10 | 17,616.74 | 0.00303 |
| 11 | 17,615.18 | 0.00302 |
| 12 | 17,615.98 | 0.00298 |
| 13 | 17,615.54 | 0.00388 |
| 14 | 17,616.48 | 0.00288 |
| 15 | 17,615.25 | 0.00248 |
| 16 | 17,616.48 | 0.00317 |
| 17 | 17,616.78 | 0.00338 |
| 18 | 17,615.38 | 0.00278 |
| 19 | 17,616.88 | 0.00248 |
| 20 | 17,615.18 | 0.00378 |
| Average | 17,616.12 | 0.00314 |

17,615.54 psi and maximum deflection 0.00356 in. that are presented, respectively, in Figs. 9.14 and 9.15 by computer-aided modeling and numerical simulation.

Table 9.6 demonstrates the prototype testing results of base support of carton top closer unit in this new automated and high-speed packaging machinery system.

The prototype experimental results for base support of carton top closer unit in Table 9.6 prove the normal function as the average maximum stress 17,354.02 psi and average maximum deflection 0.00468 in. are almost same as the results of maximum stress 17,354.47 psi and maximum deflection 0.00427 in. that are represented, respectively, in Figs. 9.17 and 9.18 by computer-aided modeling and numerical simulation.

Table 9.7 expresses the prototype testing results of tension mechanism of carton top closer unit in this new automated and high-speed packaging machinery system.

The prototype experimental results for tension mechanism of carton top closer unit in Table 9.7 verify the proper function because the average maximum stress 17,270.49 psi and average maximum deflection 0.00375 in. are approximately equal to the results of maximum stress 17,270.99 psi and maximum deflection 0.00340 in. that are indicated, respectively, in Figs. 9.19 and 9.20 by computer-aided modeling and numerical simulation.

Table 9.8 records the prototype testing results of offloading unit in this new automated and high-speed packaging machinery system.

**Table 9.6** Prototype testing of base support of carton top closer unit in this new automated and high-speed packaging machinery system

| Number of experiment | Maximum stress (psi) | Maximum deflection (in.) |
|---|---|---|
| 1 | 17,354.08 | 0.00477 |
| 2 | 17,354.68 | 0.00408 |
| 3 | 17,353.75 | 0.00487 |
| 4 | 17,353.55 | 0.00498 |
| 5 | 17,354.54 | 0.00418 |
| 6 | 17,353.66 | 0.00499 |
| 7 | 17,353.48 | 0.00495 |
| 8 | 17,354.08 | 0.00498 |
| 9 | 17,354.11 | 0.00418 |
| 10 | 17,354.54 | 0.00496 |
| 11 | 17,353.57 | 0.00498 |
| 12 | 17,354.12 | 0.00408 |
| 13 | 17,354.88 | 0.00498 |
| 14 | 17,353.48 | 0.00492 |
| 15 | 17,353.38 | 0.00499 |
| 16 | 17,354.78 | 0.00419 |
| 17 | 17,353.55 | 0.00487 |
| 18 | 17,353.48 | 0.00489 |
| 19 | 17,354.18 | 0.00418 |
| 20 | 17,354.55 | 0.00448 |
| Average | 17,354.02 | 0.00468 |

**Table 9.7** Prototype testing of tension mechanism of carton top closer unit in this new automated and high-speed packaging machinery system

| Number of experiment | Maximum stress (psi) | Maximum deflection (in.) |
|---|---|---|
| 1 | 17,270.89 | 0.00395 |
| 2 | 17,270.18 | 0.00388 |
| 3 | 17,271.08 | 0.00339 |
| 4 | 17,270.24 | 0.00398 |
| 5 | 17,270.08 | 0.00385 |
| 6 | 17,271.05 | 0.00396 |
| 7 | 17,270.19 | 0.00338 |
| 8 | 17,270.25 | 0.00336 |
| 9 | 17,270.38 | 0.00399 |
| 10 | 17,271.08 | 0.00397 |
| 11 | 17,270.18 | 0.00338 |
| 12 | 17,270.27 | 0.00399 |
| 13 | 17,270.08 | 0.00387 |
| 14 | 17,271.02 | 0.00398 |
| 15 | 17,270.05 | 0.00339 |
| 16 | 17,270.12 | 0.00338 |
| 17 | 17,270.08 | 0.00398 |
| 18 | 17,271.05 | 0.00394 |
| 19 | 17,270.48 | 0.00398 |
| 20 | 17,271.05 | 0.00337 |
| Average | 17,270.49 | 0.00375 |

**Table 9.8** Prototype testing of offloading unit in this new automated and high-speed packaging machinery system

| Number of experiment | Maximum stress (psi) | Maximum deflection (in.) |
|---|---|---|
| 1 | 17,964.25 | 0.00624 |
| 2 | 17,964.55 | 0.00638 |
| 3 | 17,963.48 | 0.00618 |
| 4 | 17,964.18 | 0.00584 |
| 5 | 17,963.38 | 0.00602 |
| 6 | 17,964.12 | 0.00608 |
| 7 | 17,963.24 | 0.00579 |
| 8 | 17,964.54 | 0.00601 |
| 9 | 17,963.21 | 0.00635 |
| 10 | 17,964.48 | 0.00575 |
| 11 | 17,964.24 | 0.00584 |
| 12 | 17,963.18 | 0.00603 |
| 13 | 17,964.42 | 0.00608 |
| 14 | 17,964.11 | 0.00579 |
| 15 | 17,963.23 | 0.00601 |
| 16 | 17,964.78 | 0.00603 |
| 17 | 17,963.11 | 0.00566 |
| 18 | 17,964.68 | 0.00575 |
| 19 | 17,963.48 | 0.00602 |
| 20 | 17,964.54 | 0.00638 |
| Average | 17,963.96 | 0.00601 |

The prototype experimental results of offloading unit in Table 9.8 confirm the appropriate function since the average maximum stress 17,963.96 psi and average maximum deflection 0.00601 in. are approximately same as the results of maximum stress 17,964.43 psi and maximum deflection 0.00631 in. that are laid out, respectively, in Figs. 9.22 and 9.23 by computer-aided modeling and numerical simulation.

Table 9.9 states the prototype testing results of rejecting unit in this new automated and high-speed packaging machinery system.

The prototype experimental results of rejecting unit in Table 9.9 prove the normal function as the average maximum stress 17,984.53 psi and average maximum deflection 0.00455 in. are close to the results of maximum stress 17,984.14 psi and maximum deflection 0.00421 in. that are shown, respectively, in Figs. 9.25 and 9.26 by computer-aided modeling and numerical simulation.

**Table 9.9** Prototype testing of rejecting unit in this new automated and high-speed packaging machinery system

| Number of experiment | Maximum stress (psi) | Maximum deflection (in.) |
|---|---|---|
| 1 | 17,984.24 | 0.00438 |
| 2 | 17,984.84 | 0.00418 |
| 3 | 17,984.02 | 0.00455 |
| 4 | 17,984.18 | 0.00477 |
| 5 | 17,984.88 | 0.00495 |
| 6 | 17,984.95 | 0.00411 |
| 7 | 17,984.98 | 0.00488 |
| 8 | 17,984.09 | 0.00459 |
| 9 | 17,983.88 | 0.00411 |
| 10 | 17,984.48 | 0.00484 |
| 11 | 17,984.77 | 0.00488 |
| 12 | 17,984.05 | 0.00418 |
| 13 | 17,984.78 | 0.00415 |
| 14 | 17,984.95 | 0.00479 |
| 15 | 17,984.88 | 0.00499 |
| 16 | 17,984.08 | 0.00448 |
| 17 | 17,984.68 | 0.00415 |
| 18 | 17,984.97 | 0.00484 |
| 19 | 17,984.78 | 0.00498 |
| 20 | 17,984.08 | 0.00419 |
| Average | 17,984.53 | 0.00455 |

## 9.4 Discussion and Future Improvement on Automated and High-Speed Packaging Machinery Systems

Automated packaging machines are the multi-axis mechanical systems that require multiple interacting mechanisms to manipulate the components for final product packages. It can help industry to minimize unnecessary human involvement, reduce labor cost, improve packing quality, and increase productivity. The technology improvement helps developing and making the automatic packing machine simpler and more precised for accurate and flexible automatic packing operations. Future improvement will focus on modifying this new system for quick changeover on different product packing, easier tool and fixture adjustment, continuous workflow maintenance, consistent production line balance, and simple equipment installation.